



Experimental and Computational approaches to the molecular structure of Myristicin - a biologically active compound of Nutmeg

J.Sherin Percy Prema Leela^{1*}, R.Hemamalini² and S. Muthu³

¹Department of Electronic Science, JBAS College for women, Tamilnadu, India

²PG & Research Department of Physics, Queen Mary's College, Tamilnadu, India

³Department of Physics, Arignar Anna Govt Arts College, Cheyyar 604407, India

Abstract : Nutmeg (*Myristica fragrans*) is a spice plant belonging to Myristicaceae family. The main chemical components of Nutmeg are camphene, safrole, methyl eugenol and myristicin, which provide the spice its therapeutic properties. Myristicin (6-allyl-4-methoxy-1,3-benzodioxole) a crystalline phenolic ether $C_{11}H_{12}O_3$ is major active constituent of nutmeg which is reported to have the anti-inflammatory, antidiabetic, antihyperlipidemic, anti-diarrheal activity. The vibrational frequencies were calculated and compared with the experimental data by using the spectroscopic methods and Density Functional Theory (DFT) method with B3LYP6-311++G(d,p) basis set. Stability of the molecule arising from hyper conjugative interactions, charge delocalization has been analyzed using natural bond orbital (NBO) analysis. In addition, the calculated HOMO and LUMO energies and molecular electrostatic potential shows that charge transfer occurs in the molecule.

Key words : Density Functional Theory method (DFT), Natural bond orbital analysis (NBO), Highest Occupied Molecular Orbital (HOMO) and Lowest Unoccupied Molecular Orbital (LUMO).

1. Introduction

The Ayurvedic system of medicine mainly uses herbs, herbal products, in the form of dried powders, extracts, kashayas, asavas, aristas etc. These formulations usually contain more than one type of herb or herbal products. The nutmeg tree biologically termed as *Myristica fragrans* is important for two spices derived from the fruit, they are the Nutmeg and mace. Nutmeg is the seed kernel inside the fruit and mace is the red lacy covering (aril) on the kernel. The seeds of this plant have been reported to possess analgesic and anti-inflammatory properties¹, preventing hypercholesterolemia² and atherosclerosis, Crude extract of nutmeg has chemopreventive and anti *Helicobacter pylori* activities³, major essential oils of nutmeg⁴, possess extraordinarily potent hepatoprotective activity⁵. Myristicin (6-allyl-4-methoxy-1,3-benzodioxole) is a natural organic compound with chemical formula is $C_{11}H_{12}O_3$ present in small amounts in the essential oil of nutmeg and to a

lesser extent, in other spices such as parsley and dill showing activity against selected leukemia lines and (RD) cancer cell lines⁶. Owing to the broad spectrum of biological activities of the drug, we have attempted to isolate, characterize and confirm spectroscopically its structure. The literature survey reveals that to the best of our knowledge, no experimental and computational spectroscopic study was performed. In this case, the aim of this study is to present a detailed description of the 6-allyl-4-methoxy-1,3-benzodioxole molecule by using both computational (Gaussian 03W program -Becke's three-parameter hybrid functional⁷(B3LYP)6-311++G(d,p) basis sets) and experimental techniques (FT-IR and FT-Raman), potential energy distribution (PED), redistribution of electron density (ED) in various bonding, antibonding orbitals and $E_{(2)}$ energies⁸, to provide evidence of stabilization originating from the hyper conjugation and various intra-molecular interactions. HOMO-LUMO analysis has been used to elucidate information regarding charge transfer within the molecule.

2. Experimental

Nutmeg collected from the local markets of Chennai, Tamil Nadu, India was dried ground and powdered with the help of mortar and pestle. 20 g of sample was mixed with 100 ml of ethanol. Extracts were made using rotary shaker soxhlet apparatus (for 6 hours at 70°C) and were cooled, filtered and evaporated using hot air oven to near dryness at 65- 70°C. Extracts (Myristicin) were placed in dark glass bottles and stored at 4°C until further analysis. The FTIR spectrum of the freshly prepared Myristicin belonging to C_1 point group symmetry was recorded in the region 4000–400 cm^{-1} using Bruker IFS 66V Spectrometer and FT-Raman spectrum, using Bruker RFS 27 Spectrometer and UV spectrum in the range 200-800 nm using JASCO V-660 spectrophotometer at CLRI, Chennai.

3. Results and Discussion

I. Vibrational Assignment-FTIR, FT Raman

The 6-allyl-4-methoxy-1,3-benzodioxole molecule has 26 atoms (fig 1) and 36 normal vibrational modes, which are found to be active in both IR and Raman scattering simultaneously as shown in figs 2 and 3 and compared vibration frequencies are presented in Table 1.

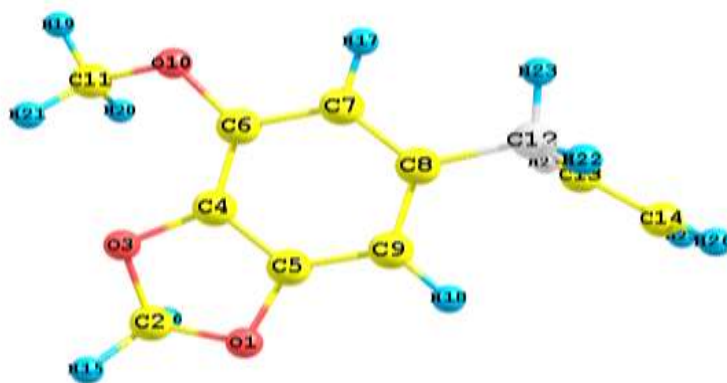


Fig. 1 Molecular structure with atom numbering scheme of 6-allyl-4-methoxy-1,3-benzodioxole.

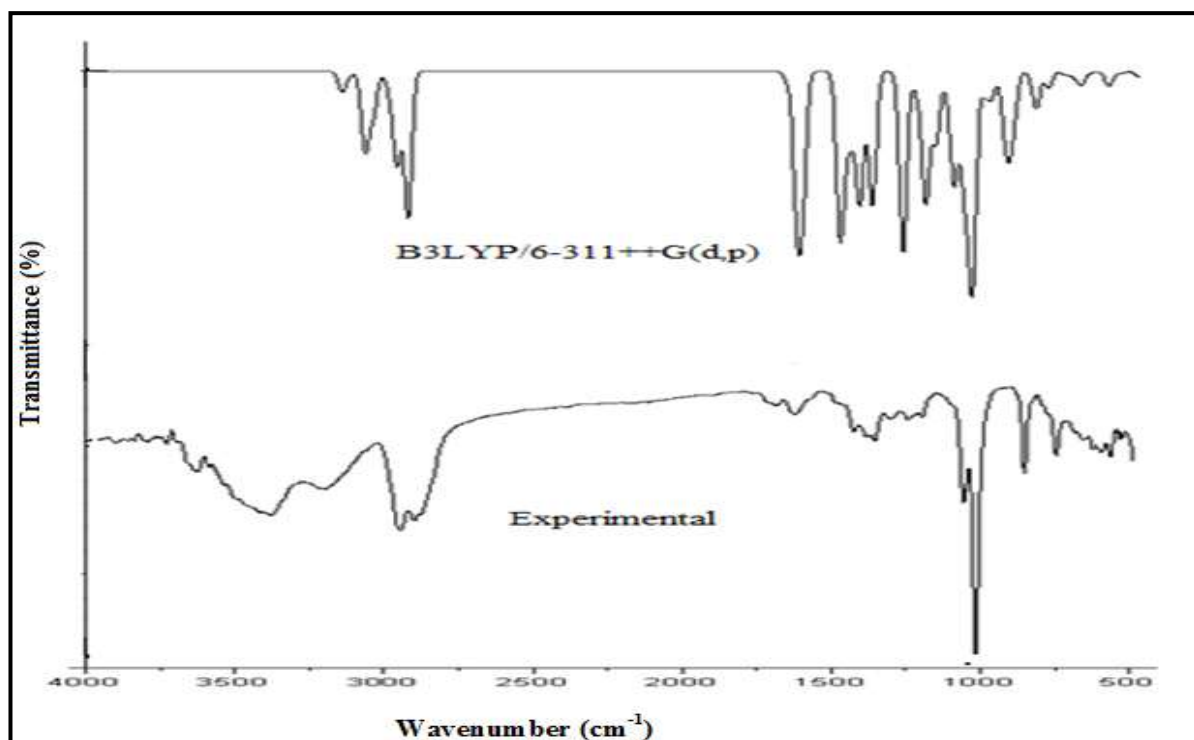


Fig.2 FT-IR spectra of Myristicin (A) Experimental (B)B3LYP/6-31++G(d,p)

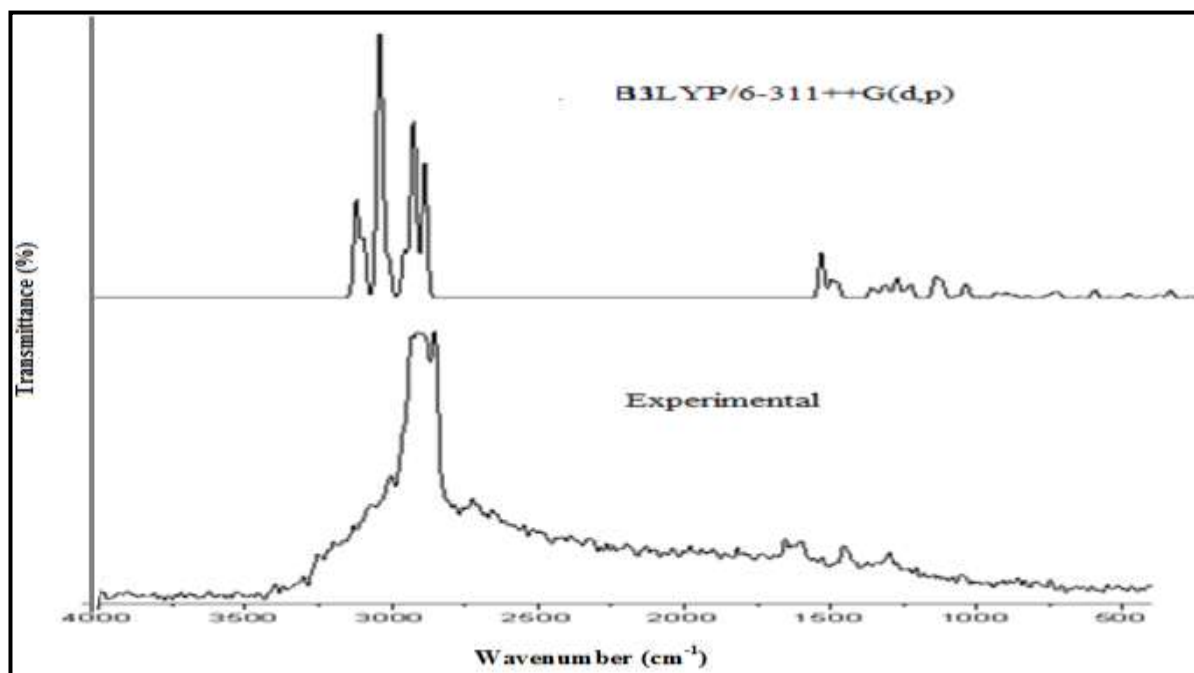


Fig 3 FT-Raman spectra of Myristicin (A) Experimental (B)B3LYP/6-31++G(d,p)

Table 1 Vibrational wavenumbers obtained for Myristicin

Experimental wave number cm^{-1}		Theoretical wave number cm^{-1}	FT-IR		FT-Raman		Assignment of vibrational modes (PED %)
FT-IR	FT-Raman		Relative	Absolute	Relative	Absolute	
	3066	3083	16	9	94	46	$\gamma\text{CH}(97)$
		3078	1	0	64	31	$\gamma\text{CH}(100)$

Experimental wave number cm^{-1}		Theoretical wave number cm^{-1}	FT-IR		FT-Raman		Assignment of vibrational modes (PED %)
FT-IR	FT-Raman	Scaled	Relative	Absolute	Relative	Absolute	
		3059	3	2	85	41	$\gamma\text{CH}(100)$
		3014	19	11	114	55	$\gamma\text{CH}(97)$
		3008	5	3	135	65	$\gamma\text{CH}(93)$
		3007	32	18	155	75	$\gamma\text{CH}(96)$
	3001	3000	15	9	53	26	$\gamma\text{CH}(100)$
2972		2980	30	17	58	28	$\gamma\text{CH}(93)$
2925		2932	12	7	72	35	$\gamma\text{CH}(99)$
	2911	2908	58	33	168	81	$\gamma\text{CH}(100)$
	2724	2898	24	14	150	73	$\gamma\text{CH}(99)$
	2658	2868	119	69	207	100	$\gamma\text{CH}(96)$
1653	1654	1631	110	63	27	13	$\gamma\text{CC}(56)$
	1598	1581	97	56	22	11	$\gamma\text{CC}(58)$
	1529	1474	3	1	14	7	$\beta\text{HCH}(87)$
1451	1455	1459	129	74	5	3	$\gamma\text{CC}(34), \text{HCC}(26)$
	1440	1442	22	13	6	3	$\beta\text{HCH}(76), \tau\text{HCOC}(12)$
	1432	1434	8	5	12	6	$\beta\text{HCH}(68), \tau\text{HCOC}(14)$
		1425	26	15	5	2	$\beta\text{HCH}(59)$
		1419	21	12	6	3	$\beta\text{HCH}(80)$
		1396	70	40	21	10	$\beta\text{HCH}(32)$
1381		1392	37	21	10	5	$\beta\text{HCH}(45)$
		1369	11	6	9	4	$\tau\text{HCOC}(64)$
1332		1353	106	61	20	10	$\gamma\text{CC}(40)$
1270	1299	1276	2	1	29	14	$\gamma\text{CC}(16), \beta\text{HCH}(1), \beta\text{HCC}(37), \text{HCCC}(12)$
		1262	1	0	12	6	$\beta\text{HCC}(33), \tau\text{HCCC}(41)$
		1253	148	85	18	8	$\gamma\text{CC}(33), \gamma\text{OC}(12)$
	1207	1210	15	9	3	2	$\beta\text{HCC}(64)$
		1183	10	6	9	4	$\beta\text{HCO}(29), \beta\text{HCC}(17), \tau\text{HCOC}(18)$
		1181	78	45	6	3	$\beta\text{HCH}(12), \tau\text{HCOC}(46)$
		1176	23	13	8	4	$\tau\text{HCO}(20), \beta\text{HCC}(29), \tau\text{HCOC}(12)$
		1147	58	33	1	1	$\gamma\text{OC}(12), \beta\text{CCC}(14), \beta\text{HCC}(13)$
		1124	3	2	2	1	$\beta\text{HCH}(28), \tau\text{HCOC}(69)$
		1104	15	8	0	0	$\beta\text{HCO}(24), \beta\text{COC}(10), \tau\text{HCOC}(33), \tau\text{COCC}(10)$
1083		1087	77	44	4	2	$\gamma\text{OC}(23), \gamma\text{CC}(12)$
		1079	14	8	5	2	$\gamma\text{CC}(15), \beta\text{HCC}(18), \tau\text{HCCC}(15)$
1042	1055	1053	91	52	8	4	$\gamma\text{OC}(16), \beta\text{OCC}(13)$
		1027	174	100	4	2	$\gamma\text{OC}(29), \beta\text{OCC}(22)$
878		990	17	10	3	1	$\tau\text{HCCC}(81)$
		965	21	12	1	1	$\gamma\text{OC}(58)$
		927	13	7	3	1	$\gamma\text{CC}(26), \gamma\text{OC}(17)$
		918	27	16	0	0	$\gamma\text{OC}(24), \beta\text{OCC}(10), \beta\text{COC}(12)$
		909	35	20	6	3	$\tau\text{HCCC}(84)$
		894	32	18	8	4	$\gamma\text{CC}(18), \tau\text{HCCC}(16)$

Experimental wave number cm^{-1}		Theoretical wave number cm^{-1}	FT-IR			FT-Raman		Assignment of vibrational modes (PED %)
FT-IR	FT-Raman	Scaled	Relative	Absolute	Relative	Absolute		
	857	882	4	2	1	0	$\beta\text{HCCC}(48)$, $\tau\text{HCCC}(13)$	
	833	834	2	1	0	0	$\tau\text{HCCC}(79)$	
		819	30	17	2	1	$\tau\text{HCCC}(69)$	
772	798	778	14	8	12	6	$\gamma\text{CC}(11)$, $\gamma\text{OC}(25)$, $\beta\text{CCC}(14)$	
	747	724	3	2	2	1	$\gamma\text{CC}(10)$, $\beta\text{OCC}(33)$, $\beta\text{COC}(21)$	
	709	696	4	2	0	0	$\gamma\text{CCCC}(39)$, $\text{OUTOCCC}(39)$	
647		672	11	7	6	3	$\tau\text{HCCC}(14)$	
622		638	1	1	2	1	$\beta\text{CCC}(23)$, $\beta\text{OCC}(10)$, $\beta\text{COC}(11)$	
		584	11	6	3	2	$\tau\text{HCCC}(11)$, $\tau\text{CCCC}(18)$, $\text{OUTCCCC}(24)$, $\text{OUTOCCC}(11)$	
		571	2	1	3	1	$\text{OUTOCCC}(52)$	
	552	541	2	1	11	5	$\gamma\text{CC}(11)$, $\gamma\text{OC}(11)$, $\beta\text{CCC}(15)$	
	461	485	4	2	2	1	$\beta\text{CCC}(31)$, $\beta\text{OCC}(10)$	

The aromatic C–H stretching, C–H in plane bending and C–H out of plane bending vibrations appear in $3000\text{--}3100\text{ cm}^{-1}$, $1100\text{--}1500\text{ cm}^{-1}$ and $800\text{--}1000\text{ cm}^{-1}$ frequency ranges, respectively⁹. The 6-allyl-4-methoxy-1,3-benzodioxole stretching ring vibrations are predicted at $3083\text{--}3000\text{ cm}^{-1}$ for B3LYP/6-311++G(d,p) level of theory. These vibrations observed experimentally at 3066 and 3001 cm^{-1} in the FT-IR spectrum were due to the C-H symmetric stretching. The scaled theoretical values of ring C-H stretching modes coincide well with that of experimental data as depicted in Table 1. The percentage of PED predicts that C-H modes of the title compound are very pure, since their percentage is almost 100%. The bands at 2972 cm^{-1} and 2925 cm^{-1} in the FT-IR spectrum and the strong bands observed at 2911 , 2824 and 2858 cm^{-1} in the FT-Raman spectrum were due to the C-H asymmetric stretching and presence of a methoxy group (O-CH_3) in the fourth position of the benzene ring. The in-plane bending observed at 1529 in FT Raman with 87% PED are well matched the calculated wavenumber. The out-of-plane bending vibrations have been calculated at 1442 , 1434 , 1425 and 1419 cm^{-1} in B3LYP method and correlated with FT Raman at 1440 and 1432 cm^{-1} . The absorption is sensitive for both the carbon and oxygen atoms of the carbonyl group. Normally, the C–O stretching vibrations occur in the region $1260\text{--}1000\text{ cm}^{-1}$. In the present study, the C–O stretching vibration is assigned at calculated wavenumbers between 1147 and 1027 cm^{-1} showing good agreement with experimental FTIR spectral region at 1083 cm^{-1} , 1042 cm^{-1} and 1055 cm^{-1} in FT-Raman spectral region respectively. These assignments are in agreement with the literature values¹⁰.

ii. UV Visible Spectroscopic Analysis

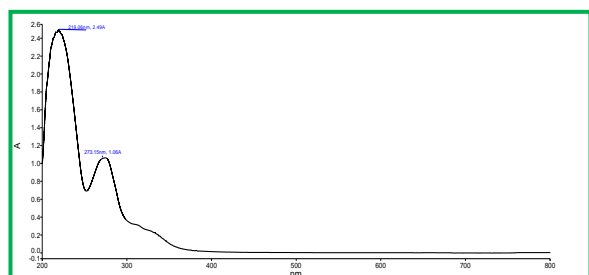


Fig. 4 UV-VIS spectrum of Myristicin

A substituent, typically methyl, hydroxyl, alkoxy or amino group or an atom of halogen in a benzene ring increases absorption of a molecule, when the auxochrome is conjugated with a π -electron system, the λ_{\max} value is shifted to a longer wavelength. A methoxy substitution is likely to show absorption peak at 270 nm. The Cl-M-DPQ in THF solution exhibits an absorption with a λ_{\max} at 270 nm, due to $\pi - \pi^*$ transition contributed by the methoxy conjugated quinoline backbone¹¹. Myristicin UV spectrum (fig 4) shows two significant peaks at 219 and 273 nm. The peaks are associated with vibrational effects on $\pi \rightarrow \pi^*$ transitions in the allyl group and methoxy group. The methoxy and allyl groups are sandwiched chromophores on either side of the benzodioxole group in myristicin thus giving rise to significant transitions accounting for the UV absorption maxima at 219 and 273 nm.

iii. NBO analysis

Natural bond orbital analysis provide an efficient method for studying intra and inter molecular bonding and interaction among bonds in both filled and virtual orbital spaces and provides a convenient basis for investigating charge transfer or conjugative interaction in molecular systems¹². The second-order Fock matrix was carried out to evaluate the donor-acceptor interactions in NBO analysis. For each donor (i) and acceptor (j), the stabilization energy E_2 associated with the delocalization $i \rightarrow j$ is estimated as

$$E_2 = \Delta E_{ij} = \frac{q_i (F_{ij})^2}{\epsilon_j - \epsilon_i}$$

where q_i is the donor orbital occupancy, ϵ_j and ϵ_i are diagonal elements and F_{ij} is the off diagonal NBO Fock matrix element. The stabilization energy $E_{(2)}$ (Table 2) associated with the hyper conjugative interactions viz. σ (C13-C14) $\rightarrow \sigma^*$ (C13-H24), σ^* (C14-H25) are obtained at 25.22 kJ/mol and σ (C14-H26) $\rightarrow \sigma^*$ (C13-H14), σ^* (C13-H24), σ^* (C14-H25) at 60.41 kJ/mol. The other hyper conjugate interactions of LP (2) of O1 $\rightarrow \pi^*$ (C5-C9), LP (2) of O3 $\rightarrow \pi^*$ (C4-C6) with stabilization energies 39.04, 43.44 kJ/mol respectively. The most significant interaction energy, related to the resonance in the molecule, is the electrons donating from antibonding donor π^* (C4-C6), π^* (C5-C9) to the antibonding acceptor π^* (C7-C8), π^* (C7-C8) with large stabilization energy of 206.15, 227.74 kJ/mol respectively. The larger the $E(2)$ (energy of hyper conjugative interactions) value, the more intensive is the interaction between electron donors and electron acceptors, i.e. the more donating tendency from electron donors to electron acceptors, the greater the extent of conjugation of the whole system.

Table. 2 Second order perturbation theory analysis of fock matrix in NBO basis

Donor (i)	Type	ED/e	Acceptor (j)	Type	ED/e	^a E ⁽²⁾ (kJ/mol)	^b E(j) - E(i) (a.u)	^c F(i,j) (a.u)
C4-C6	π	1.67022	C5-C9	π^*	0.44259	24.28	0.33	0.082
C5-C9	π	1.68688	C7-C8	π^*	0.39009	24.77	0.33	0.082
C7-C8	π	1.70174	C4-C6	π^*	0.453	25.61	0.29	0.08
C13-C14	σ	1.98951	C13-H24	σ^*	0.02799	25.22	3.47	0.265
C14-H26	σ		C13-H24	σ^*	0.02799	28.03	3.22	0.269
C14-H26	σ		C14-H25	σ^*	0.02799	60.41	4.75	0.479
O1	LP(2)		C5-C9	π^*	0.44259	43.44	0.41	0.127
O3	LP(2)		C4-C6	π^*	0.453	39.04	0.4	0.121
O10	LP(2)	1.86114	C4-C6	π^*	0.453	27.07	0.35	0.095
C4-C6	π^*	0.453	C7-C8	π^*	0.39009	206.15	0.02	0.09
C5-C9	π^*	0.44259	C7-C8	π^*	0.39009	227.74	0.02	0.092

iv HOMO-LUMO analysis

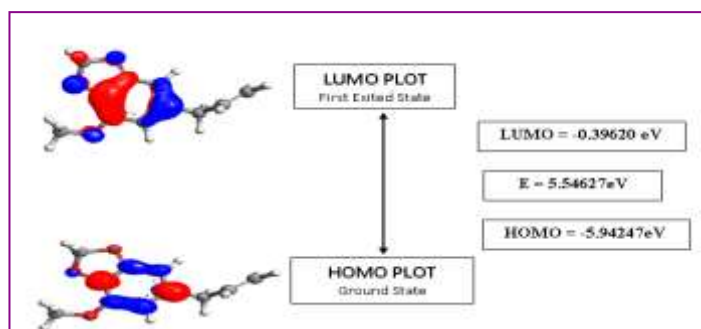


Fig 5 Highest Occupied and Lowest Unoccupied Molecular Orbitals

Owing to the interaction between Highest Occupied and Lowest Unoccupied Molecular Orbitals (HOMO and LUMO) orbital of a structure, transition state of $\pi \rightarrow \pi^*$ type is observed with regard to the molecular orbital theory¹³. The frontier orbital gap helps characterize the chemical reactivity and the kinetic stability of the molecule. The HOMO and LUMO energy gap for 6-allyl-4-methoxy-1,3-benzodioxole (Fig 5) is 5.54627 eV. The narrow energy gap, small frontier orbital gap facilitates high chemical reactivity and low kinetic stability and is also termed as soft molecule¹⁴.

v. Molecular electrostatic potential

Molecular electrostatic potential have been found to be a very useful tool in investigation of correlation between molecular structures with its physiochemical property relationship, including biomolecules and drugs¹⁵. The different electrostatic potential values of the surface are represented by different colors¹⁶. The maximum negative region, which is the preferred site for electrophilic reactivity (oxygen) is shown in red region in the MEPS fig. 6, the maximum positive region (hydrogen), for nucleophilic reactivity in white represent the zero potentials.

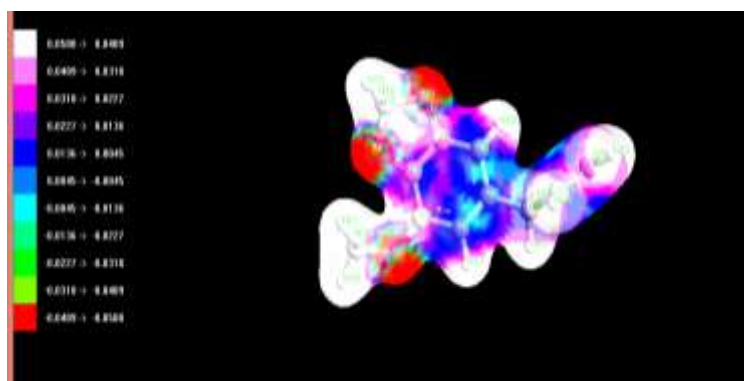


Fig 6 Molecular electrostatic potential (MEP) and Contour map of title compound

4. Conclusion

In the present work, the optimized molecular structure, vibrational frequencies, intensity of vibrations of myristicin have been calculated by DFT method. The vibrational FT-IR and FT-Raman spectra exhibit good agreement between the calculated and experimental results. The assignments of all the fundamental vibrational modes have been made unambiguously based on the results of the PED output obtained from normal coordinate analysis. The MEP map contour shows that the negative potential sites are on electronegative oxygen atoms as well as the positive potential sites are around the hydrogen atoms. The movement of π -electron cloud from donor to acceptor i.e. intramolecular charge transfer can make the molecule more polarized and the Natural bond orbital (NBO) calculations reveals the delocalization and hyperconjugation interaction, intramolecular charge transfer and stabilization energy of molecule and the HOMO-LUMO energy gap is responsible for the NLO properties of molecule. It is henceforth established that the title molecule is an attractive object for future studies on non-linear optical properties for the application in Pharmaceutical industries and fundamental researches in chemistry and biology.

Reference

1. Olajide OA, Ajayi FF, Ekhelar AI, Awe SO, Makinde JM, Alada AR, Biological effects of Myristica fragrans fruits extract in rabbits, *Phytother Res.*,1999,13(4),344-345.
2. Somani RS, Singhai AK, Hypoglycaemic and antidiabetic activities of seeds of Myristica fragrans in normoglycaemic and Alloxan-induced diabetic rats, *Asian J. Exp. Sci.*, 2008,22(1), 95-102.
3. Bhamarapravati S, Pendland SL, Mahady GB,Extracts of spice and food plants from Thai traditional medicine inhibit the growth of the human carcinogen Helicobacter pylori, *In Vivo* 2003,17(6), 541-4.
4. Mohd Abdul Rasheed Naikodi, Mohd Abdul Waheed, Mohammad Ataulah Shareef, Mushtaq Ahmad, and Kommu Nagaiah, Standardization of the Unani drug Myristica fragrans Houtt (Javetri) *Pharmaceutical Methods*, 2011, 2(2), 76-82.
5. Morita T, Jinno K, Kawagishi H, Arimoto Y, Suganuma H, Inakuma T, Sugiyama.K, Hepatoprotective Effect of Myristicin from Nutmeg (Myristica fragrans) on Lipopolysaccharide / d-Galactosamine-Induced Liver Injury, *J Agric Food Chem*, 2003,51,1560-5.
6. Essam F. Al-Jumaily and Aseel Jameel Al-Massody Cytogenetic study of the pure Myristicin from Nutmeg (Myristica Fragrans) on Rhabdomyosarcoma Cell Line (In Vitro) *DAV International Journal of Science*, 2012, 1(2),2277-5536.
7. FrischM.J., et al., Gaussian 03, Revision B.01, Gaussian Inc., Pittsburgh, PA 2003.
8. Glendening.E.D, Reed. A.E, Carpenter. J.E, Weinhold.F, NBO Version 3.1, Tcl,University of Wisconsin, Madison, 1998.
9. Vrielynck.L, Cornard. J.P, Merlin.J.C,Lautie. M.F, Semi-empirical and vibrational studies of flavone and some deuterated analogues, *Spectrochim. Acta* 1994,50,2177–2188.
10. Snehatatha.M, Ravikumar.C, Joe.I.H, Sekar.N, Jayakumar.V.S, Spectroscopic analysis and DFT calculations of a food additive Carmoisine, *Spectrochim. Acta Part A*, 2009,72,654-662.
11. Zade.G, Dhoble.S, Raut.S and Pode.R, Synthesis and Characterization of Chlorine-methoxy-diphenylquinoline (Cl-MO-DPQ) and Chlorine-methyl-diphenylquinoline (Cl-M-DPQ) Blue Emitting Organic Phosphors," *Journal of Modern Physics*,2011,2(12),1523-1529.
12. Reed.A.E, Weinhold.R.B, Weinhold.F, *J. Chem. Phys.*,1985, 83,735.
13. Fukui.K, *Theory of Orientation and Stereo Selection*, Springer-Verlag, Berlin,1975.
14. Fleming, *Frontier Orbitals and Organic Chemical Reactions*, Wiley, London, 1976.
15. Murray.J.S, Sen.K, *Molecular Electrostatic Potentials Concepts and Applications*, Elsevier, Amsterdam, 1996.
16. Scrocco.E, Tomasi.T, Electronic molecular structure, reactivity and intermolecular forces, an euristic interpretation by means of electrostatic molecular potentials, *Adv. Quantum Chem*,1978, 11,115–121.
